Contents lists available at ScienceDirect

International Journal of Engineering Science

journal homepage: www.elsevier.com/locate/ijengsci

Modeling pull-in instability of CNT nanotweezers under electrostatic and van der Waals attractions based on the nonlocal theory of elasticity

Gennadi Mikhasev [a], Enrico Radi [b,*], Vyacheslav Misnik [c]

[a] Harbin Institute of Technology, 92 West Dazhi Street, Nangang District, 150001 Harbin, China
[b] Dipartimento di Scienze e Metodi dell'Ingegneria, Università di Modena e Reggio Emilia, Via Amendola 2, Reggio Emilia, 42122, Italy
[c] Department of Mechanics and Mathematics, Belarusian State University, Nezavisimosti Ave. 4, Minsk 220030, Belarus

ARTICLE INFO

Keywords:
CNT nanotweezer
Pull-in instability
van der Waals attraction
Electrostatic forces
Nonlocal elasticity

ABSTRACT

This work investigates the electromechanical response and pull-in instability of an electrostati cally-actuated CNT tweezer taking into consideration a TPNL constitutive behavior of the CNTs as well as the intermolecular forces, both of which provide a significant contribution at the nanoscale. The nonlocal response of the material introduces two additional parameters in the formulation, which are effective in capturing the size effects observed at the nanoscale. The problem is governed by a nonlinear integrodifferential equation, which can be reduced to a sixth-order nonlinear ODE with two additional boundary conditions accounting for the nonlocal effects near to the CNT edges. A simplified model of the device is proposed based on the assumption of a linear or parabolic distribution of the loading acting on the CNTs. This assumption allows us to formulate the problem in terms of a linear ODE subject to two-point boundary conditions, which can be solved analytically. The results are interesting for MEMS and NEMS design. They show that strong coupling occurs between the intermolecular forces and the characteristic material lengths as smaller structure sizes are considered. Considering the influence of the nonlocal constitutive behavior and intermolecular forces in CNT tweezers will equip these devices with reliability and functional sensitivity, as required for modern engineering applications.

1. Introduction

A nanotweezer refers to a tiny, nanoscale device used to trap, manipulate, and position nanoscale objects such as nanoparticles, nanowires, or biological entities with nanometer-scale accuracy (Kim & Lieber, 1999). When subjected to external forces, such as electrostatic and van der Waals forces, the behavior and deformation of the nanotweezer and the trapped object are influenced. Accurate modeling of the behavior of a nanotweezer under electrostatic force and van der Waals (vdW) force, considering the effects of nonlocal theory of elasticity, is extremely important for simulating and understanding the manipulation of nanoscale objects using external forces and for assuring high precision and control over the nanotweezer's movements. Due to their excellent mechanical and electrical properties, CNTs are often used as main components for nanotweezers.

Abbreviations: CNT, Carbon NanoTube; LDL, Linear Distributed Load; MEMS, Micro-Electro-Mechanical System; NEMS, Nano-Electro-Mechanical System; ODE, Ordinary Differential Equation; PNL, Purely NonLocal; QDL, Quadratic Distributed Load; TPNL, Two-Phase NonLocal; vdW, van der Waals

* Corresponding author.
E-mail addresses: mikhasev@hit.edu.cn (G. Mikhasev), eradi@unimore.it (E. Radi), slava.misnik@mail.ru (V. Misnik).

https://doi.org/10.1016/j.ijengsci.2023.104012
Received 24 November 2023; Received in revised form 18 December 2023; Accepted 18 December 2023

Electrostatic forces arise due to the presence of electrical charges on the nanotweezer arms and the trapped object. These forces can be attractive or repulsive depending on the charges involved. The magnitude of the electrostatic force depends on the distance between the charges, their magnitudes, and the dielectric properties of the surrounding medium. At the pull-in voltage, the nanotweezer arms become unstable and collide with each other. The occurrence of pull-in instability thus restricts the operating range of CNT nanotweezers and limits the size of the smallest objects that can be manipulated. Ensuring mechanical stability is thus essential to prevent undesired vibrations or fluctuations that could affect the manipulation process.

Van der Waals forces, on the other hand, are attractive forces that arise due to temporary fluctuations in the electron distribution of molecules. These forces are influenced by the geometry, surface properties, and intermolecular distances between the nanotweezer arms and the trapped object (Farrokhabadi et al., 2015, 2013). They may become comparable to the electrostatic forces at an interaction range of nanometers. Due to these forces, freestanding nanotweezers display an initial deflection even without any external voltage applied. Furthermore, if the van der Waals forces become stronger than the actuation forces applied to the nanotweezers, they can lead to the collapse or failure of the tweezer structure. This is particularly relevant when the separation distance between the tweezer tips becomes very small. The occurrence of adhesion can result in stiction if the tweezer tips stick to each other and have difficulty releasing them. Understanding and controlling van der Waals forces is crucial in the design and operation of nanotweezers to ensure their reliable and efficient performance.

Numerical simulations, such as finite element analysis or differential quadrature method, have been utilized to further explore the behavior of nanotweezers under electrostatic loadings (Farrokhabadi et al., 2014; Menning et al., 2022; Ramezani, 2011; Zare & Shateri, 2017). These simulations have allowed for a more detailed investigation of the stress distribution, deformation profiles, and critical conditions for pull-in or buckling. They have also provided a means to compare and validate the analytical models.

The problem of electrostatic pull-in of nanobeams and nanotweezers has been extensively studied in the field of nanomechanics and microelectromechanical systems (NEMS-MEMS). Several papers have contributed to understanding the phenomenon and have provided valuable insights into the behavior and limitations of these systems (see the review paper by Zhang et al. (2014) and references quoted therein). They have explored various aspects such as the static and dynamic behavior, the critical voltage for pull-in, the nonlinear response, and the influence of different geometric and constitutive parameters.

Many studies have employed analytical, numerical, and experimental approaches to investigate the electrostatic pull-in phenomenon. Analytical models, such as the Euler–Bernoulli beam theory or the Timoshenko beam theory, have been used to derive governing equations and expressions for the pull-in voltage and displacement (e.g., see Ramezani et al., 2007; Yang et al., 2008). These models provide simplified yet insightful representations of the system behavior.

Experimental studies have also played a crucial role in validating the theoretical and numerical findings and in understanding the real-world implications (Kim & Lieber, 1999; Lee & Kim, 2005). These studies have involved the fabrication of nanobeams and nanotweezers, precise measurements of pull-in voltages and displacements, and the characterization of their mechanical response under electrostatic forces. Experimental observations have provided important insights into the accuracy of the theoretical models and the practical limitations, such as the effects of fabrication imperfections, surface roughness, and material properties.

The experimental investigations have also shown that the classical theory of elasticity becomes inappropriate for an accurate simulation of the material behavior at the nanoscale, since it is not able to predict the size effect usually observed at this scale length (Khodabakhshi & Reddy, 2015; Li et al., 2015; Rahaeifard & Ahmadian, 2015; Zeighampour & Tadi Beni, 2014). An enhancement to the classical theory is provided by the nonlocal theory of elasticity, which takes into account the nonlocal response of materials, namely the deformation at a given point depends on the deformation at neighboring points. The use of nonlocal theory of elasticity in modeling nanobeam behavior under electrostatic loadings has been a topic of interest in the field of nanomechanics. It has proved to be effective in the simulation of the size effects (Demir & Civalek, 2017; Malikan et al., 2023; Miandoab et al., 2015; Tavakolian et al., 2019; Yang et al., 2008). By incorporating nonlocal effects into the models, these studies have shown that the behavior of nanobeams under electrostatic loadings differs from that predicted by classical local elasticity theories. They have aimed to capture the size-dependent behavior and accurately predict the mechanical response of nanobeams subjected to electrostatic forces and provided valuable insights into the importance of considering nonlocal effects at the nanoscale. Analytical models, such as Eringen's nonlocal elasticity theory or modified versions of classical beam theories, have been used to derive governing equations and expressions for the response of nanobeams. These models have provided insights into the influence of the nonlocal parameter, beam dimensions, and electrostatic loading on the nanobeam behavior.

In the present study, the two-phase nonlocal (TPNL) model of elasticity (Eringen, 1984, 2002), previously used by the authors for the analysis of the pull-in instability of cantilever nanobeams (Mikhasev et al., 2022), is employed to capture the size-dependent behavior of a nanotweezer device and to provide a more accurate description of its electromechanical response. This constitutive model for the Bernoulli–Euler type beam combines the purely nonlocal (PNL) theory of elasticity with classical elasticity, taking into account the nonlocal effects in the axial direction of a nanobeam, and does not suffer from the inconsistencies of the PNL model (Pisano et al., 2021; Romano et al., 2017; Vaccaro et al., 2021) applied for nanobeams based on the kinematic hypotheses. Therefore, the present analysis of nanotweezer systems can account for the influence of electrostatic and van der Waals forces while considering the size-dependent behavior and deformation characteristics. This allows for a more comprehensive understanding of the forces and deformations involved in nanomanipulation and the design of nanodevices like nanotweezers.

The paper is organized as follows. First, in Section 2 we introduce the physical model of the nanotweezer involving the electrostatic and van der Waals forces. In Section 3, the Bernoulli–Euler type equation is used as the initial one, and then the nonlinear integrodifferential equation governing the problem is derived according to the PNL theory of elasticity presented in Eringen (1984, 2002), which involves both local and non-local constitutive parameters. By assuming the attenuation kernel of the Helmholtz type, in Section 4 the problem is then reduced to an "equivalent" differential equation of the sixth order with two additional

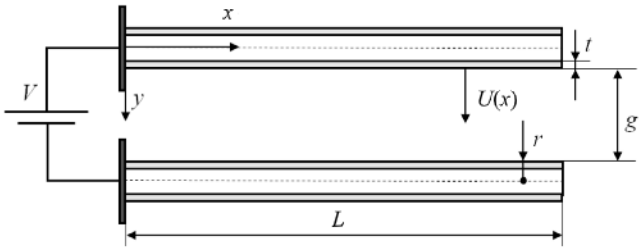

Fig. 1. CNT tweezers under electrostatic actuation.

boundary conditions accounting for nonlocal effects near the edges. As a simplifying assumption, in Section 5 the van der Waals and electrostatic forces acting on the nanotweezer arms are approximated by assuming a linear or quadratic load distribution, as in Mikhasev et al. (2022). We choose to adopt this approximation on loading instead of assuming a specific deflection shape in terms of some unknown parameters that can be determined by using the Rayleigh–Ritz method, because the governing equation involves up to the sixth-order derivatives of the deflection, while the loading function appears in it explicitly. Note also that solving the singular perturbed boundary value problem for the governing equation with a small parameter at the highest derivative, we do not perform its asymptotic splitting into the external and internal problems with layers, as was usually done when studying vibrations of nanobeams (Mikhasev, 2021; Mikhasev & Nobili, 2020) and waves in half-space (Chebakov et al., 2017; Kaplunov et al., 2023) within the framework of nonlocal elasticity theory. In Section 6, ignoring the internal nonlocal effects, we give the comparative analysis of outcomes obtained on the base of our and alternative approaches. Calculations of the free-standing tweezer length and pull-in voltage as functions of the local constitutive parameter for both load approximations are given in Section 7 and Section 8, respectively, where we also validate the assumptions on the load distribution based on the results. Finally, in Section 9, we draw some conclusions about the size effect on the pull-in voltage of nanotweezers.

Overall, the present paper on the problem of electrostatic pull-in of nanotweezers provides a significant contribution to the understanding of the underlying physics, the design considerations, and the potential applications of these systems. The development of a new and accurate analytical model allows us to achieve a deeper understanding of the electrostatic pull-in phenomenon at the nanoscale and will pave the way for further advancements in this field.

2. Physical model of CNT-based nanotweezers

We consider the typical architecture of CNT-based nanotweezers, consisting of two CNT cantilever electrodes of length L, external radius r, and wall thickness t, which are separated by an initial gap g. Menning et al. (2022) observed that the CNT atomic arrangement (armchair or zigzag) is not relevant for defining the electromechanical response of nanotweezers, which depends only on the radius and length. Let x denote the axial coordinate of each CNT ranging between 0 and L (Fig. 1).

2.1. Electrostatic forces

By applying a voltage difference V between the two electrodes, a symmetric deflection $U(x)$ of both CNTs is induced by the electrostatic attractive force per unit length, whose initial value is given by Bianchi et al. (2022) and Farrokhabadi et al. (2013)

$$F_e = \frac{\pi\varepsilon_0 V^2}{\sqrt{g^2+2gr}\left[\ln\left(1+\frac{g}{r}+\frac{g}{r}\sqrt{1+\frac{2r}{g}}\right)\right]^2}, \tag{1}$$

where ε_0 is the permittivity of the vacuum.

2.2. Van der Waals attraction

Besides the electrostatic attractive force, at the nanoscale the system is also affected by the attractive van der Waals intermolecular force, occurring for gaps smaller than 20 nm, namely (Bianchi et al., 2022; Farrokhabadi et al., 2013)

$$F_{vdW} = \frac{3At^2}{256r^{3/2}g^{5/2}}\left[1-\frac{20r}{3g}+\frac{140r^2}{3g^2}\right], \tag{2}$$

where A is the Hamaker constant.

3. Mathematical model

Here we assume that CNTs being utilized as arms of the nanotweezer have the same geometry and material properties. Then the applied voltage results in the same deflection $U(x) = U_1(x) = U_2(x)$ on both CNTs so that the deformed electromechanical system can be considered symmetric with respect to the Ox-axis. Given this circumstance, we consider the deformation of only one arm which will be modeled by the cantilever nanobeam.

The vertical equilibrium of the cantilever implies the following differential equation:

$$\frac{d^2M}{dx^2} = -q(U), \tag{3}$$

where x is the axial coordinate that is the same for both arms, M is the bending moment, and $q(U) = F_e(U) + F_{vdW}(U)$ is the resultant lateral force per unit length, which depends on the arm deflection $U(x)$ nonlinearly. As the attraction forces start acting, the gap between the CNTs decreases correspondingly. Taking into account the symmetric deformation of the system, we replace the initial gap g by the effective distance $g - 2U$, like it was done in Bianchi et al. (2022) and Farrokhabadi et al. (2013). Then the electrostatic force (1) can be rewritten as:

$$F_e(U) = \frac{\pi\varepsilon_0 V^2}{gZ(U)\left\{\ln\left[1 + \frac{g}{r}\left(1 - \frac{2U}{g} + Z(U)\right)\right]\right\}^2}, \tag{4}$$

where

$$Z(U) = \sqrt{\left(1 - \frac{2U}{g}\right)\left(1 - \frac{2U}{g} + \frac{2r}{g}\right)}. \tag{5}$$

For $r \ll g$, the van der Waals force (2) becomes

$$F_{vdW}(U) = \frac{3At^2}{256r^{3/2}(g - 2U)^{5/2}}. \tag{6}$$

The boundary conditions for the cantilever beam read

$$U(0) = U'(0) = 0, \quad M(L) = M'(L) = 0, \tag{7}$$

where prime means the derivative with respect to x.

To capture nonlocal effects in the deformed nanobeam, we use Eringen's theory of nonlocal elasticity (Eringen, 1984, 2002). In the framework of the TPNL model of elasticity, the bending moment is defined as in Mikhasev and Nobili (2020) and Mikhasev (2021)

$$M = -EI\left(\xi_1\frac{d^2U}{dx^2} + \xi_2\int_0^L K\left(|x - \hat{x}|, \kappa\right)\frac{d^2U}{d\hat{x}^2}d\hat{x}\right), \tag{8}$$

where $K\left(|x - \hat{x}|, \kappa\right)$ is a positive, symmetric kernel rapidly decaying away from x and satisfying the condition

$$\int_{\mathbb{R}} K\left(|x - \hat{x}|, \kappa\right)d\hat{x} = 1, \tag{9}$$

The nonlocal parameter $\kappa = e_0 a$ depends on the scale coefficient e_0 and the internal length scale a, ξ_1 and ξ_2 are the volume fractions representing, respectively, the local and the nonlocal phase ratios, such that $\xi_1 + \xi_2 = 1$ and $\xi_1\xi_2 \geq 0$. When $\xi_1 = 1$, the constitutive Eq. (8) degenerates into the classical local elasticity, and the case $\xi_1 = 0$ corresponds to the purely nonlocal Eringen's model.

Remark. As was mentioned in the Introduction, the constitutive equation (8) takes into account the nonlocal effects only in the axial direction. Capturing these effects in the transverse direction could be probably reached by applying TPNL model to 2D or 3D equations of elasticity, as was done in contributions (Chebakov et al., 2017; Kaplunov et al., 2023) considering waves in a half-space.

The substitution of (8) into Eq. (3) results in the following integro-differential equation

$$EI\frac{d^2}{dx^2}\left(\xi_1\frac{d^2U}{dx^2} + \xi_2\int_0^L K\left(|x - \hat{x}|, \kappa\right)\frac{d^2U}{d\hat{x}^2}d\hat{x}\right) = q(U). \tag{10}$$

4. Equivalent model in the differential form

Here we use the Helmholtz kernel

$$K\left(|x - \hat{x}|, \kappa\right) = \frac{1}{2\kappa}\exp\left(-\frac{|x - \hat{x}|}{\kappa}\right), \tag{11}$$

which is widely used for studying mechanical behavior of 1D nanosized objects (Benvenuti & Simone, 2013; Challamel & Wang, 2008; Mikhasev, 2021). The Helmholtz kernel possesses properties that allow, on the one hand, to reduce the integro-differential equation to an "equivalent" differential form, and, on the other hand, to correctly predict the bending behavior near the free edge of a nanocantilever taking into account the nonlocal effects (Mikhasev & Nobili, 2020).

First, we introduce the dimensionless variables and parameters,

$$s = \frac{x}{l}, \quad w = \frac{2U}{g}, \quad k = \frac{g}{r}, \quad \alpha = \frac{3At^2l^4}{128EIr^{3/2}g^{7/2}}, \quad \beta = \frac{2\varepsilon_0\pi V^2 l^4}{EIg^2}. \tag{12}$$

Then, assuming that $w \in C^6[0,1]$, we perform the mathematical manipulations with Eq. (10) as done in Mikhasev and Nobili (2020). As a result, we arrive at the following differential equation:

$$\mu^2\xi\frac{d^6w}{ds^6} - \frac{d^4w}{ds^4} = \mu^2\frac{d^2f(w)}{ds^2} - f(w), \tag{13}$$

where $\xi = \xi_1$, $\mu = \kappa/l$ is a small dimensionless parameter, and

$$f(w) = \frac{\alpha}{(1-w)^{5/2}} + \frac{\beta}{\sqrt{(1-w)(1-w+2/k)}\times\left[\ln\left(1+k(1-w)+k\sqrt{(1-w)(1-w+2/k)}\right)\right]^2}, \tag{14}$$

is the dimensionless sum of the van der Waals and electrostatic forces.

The boundary conditions (7) at $x = 0$ for the clamped end of the cantilever nanobeam become:

$$w(0) = w'(0) = 0. \tag{15}$$

Note that the boundary conditions (7) at $x = L$ for the free edge have the integro-differential form. However, taking into account properties of kernel (11), they can also be rewritten in the differential form, as done in Mikhasev et al. (2022):

$$\begin{aligned} &\mu^2\xi w^{IV}(1) - w''(1) - \mu^2 f(w_T) = 0, \\ &\mu^2\xi w^{IV}(1) + \mu\xi w'''(1) - (1-\xi)w''(1) - \mu^2 f(w_T) = 0, \end{aligned} \tag{16}$$

where $w_T = w(1)$ is the dimensionless deflection of the cantilever tip.

To rule out spurious solutions owing to double differentiation of the initial integro-differential equation (10), we have to introduce a pair of additional conditions called the constitutive boundary conditions (Fernandez-Saez & Zaera, 2017). Here these conditions admit the following form (Mikhasev et al., 2022):

$$\begin{aligned} &\mu^3\xi w^V(0) - \mu^2\xi w^{IV}(0) - (1-\xi)\left[\mu w'''(0) - w''(0)\right] = -\mu^2 f(0) + \mu^3 f_s'(0), \\ &\mu^3\xi w^V(1) + \mu^2\xi w^{IV}(1) - (1-\xi)\left[\mu w'''(1) + w''(1)\right] = -\mu^2 f(w_T) + \mu^3 f_s'(w_T), \end{aligned} \tag{17}$$

where $f_s' = \frac{df}{ds} = \frac{df}{dw}w'$.

We arrived at the boundary-value problem (13), (15)–(17) that depends on the dimensionless parameter β, proportional to the voltage V, the local model fraction ξ and the internal length scale parameter μ as well. Another parameter of the problem is the tip deflection w_T, which varies from 0 to 1. Due to the non-linearity of the problem, there exist such critical (minimum) values of the gap, g^*, and the voltage parameter, β^*, at which the arm tips deflect on the critical value w_T^* and then suddenly touch each other. These parameters corresponding to pull-in instability can be determined from one of the following equations:

$$\frac{d\alpha}{dw_T} = 0, \quad \frac{d\beta}{dw_T} = 0. \tag{18}$$

The first equation from (18) gives the critical value of the gap, g^*, if the electrostatic forces are absent, while the second one allows finding the critical voltage V^* with intermolecular attraction taken into account.

5. Solution method

To solve the boundary value problem set above, we apply the well-recommended approach (Mikhasev et al., 2022; Yang et al., 2008) based on the approximation of the resultant lateral force acting on the cantilever by a linear or quadratic function of the coordinate s :

$$f_n(s) = f_0 + (f_T - f_0)s^n, \tag{19}$$

where $n = 1$ or $n = 2$ depending on the assumed geometrical parameters and the local model fraction ξ (Mikhasev et al., 2022), and

$$f_0 = f(0), \quad f_T = f(w_T). \tag{20}$$

5.1. Linear distribution of resultant forces

First, consider the linear distributed load (LDL) model, when $n = 1$ in (19). In this case, the general solution of Eq. (13) for $f(w) = f_1(w)$ is readily written out (Mikhasev et al., 2022):

$$w = \sum_{k=0}^{5} c_k s^k + a_4 e^{\frac{s}{\mu\sqrt{\xi}}} + a_5 e^{-\frac{s}{\mu\sqrt{\xi}}}, \tag{21}$$

where

$$\begin{aligned} &c_0 = \mu^2\xi\left(\mu^2\xi f_0 - a_2\right) - a_0, \qquad c_1 = \mu^2\xi\left[\mu^2\xi(f_T - f_0) - a_3\right] - a_1, \qquad c_2 = \frac{1}{2}\left(\mu^2\xi f_0 - a_2\right), \\ &c_3 = \frac{1}{6}\left[\mu^2\xi(f_T - f_0) - a_3\right], \qquad c_4 = \frac{1}{24}f_0, \qquad c_5 = \frac{1}{120}(f_T - f_0). \end{aligned} \tag{22}$$

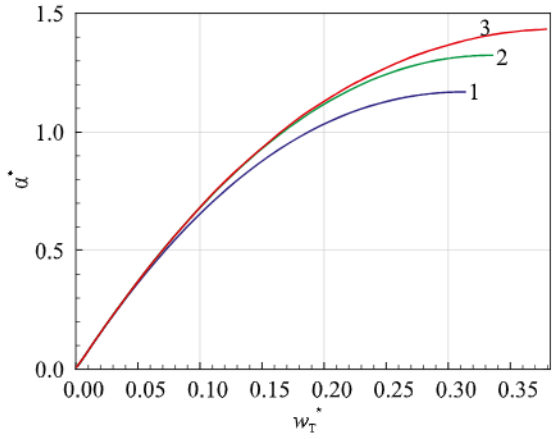

Fig. 2. The critical value of the vdW parameter α^* versus the tip deflection w_T^* obtained on the base of the LDL and QDL models (blue and green lines denoted as 1 and 2, respectively) and from the shooting method (red line denoted by 3) (Bianchi et al., 2022) for classical elastic behavior of the nanocantilever.

5.2. Quadratic distribution of resultant forces

For the quadratic distributed load model with $n = 2$ in (19), the general solution of Eq. (13) for $f(w) = f_2(w)$ is the function (Mikhasev et al., 2022)

$$w = \sum_{k=0}^{6} c_k s^k + a_4 \mathrm{e}^{\frac{s}{\mu\sqrt{\xi}}} + a_5 \mathrm{e}^{-\frac{s}{\mu\sqrt{\xi}}} \tag{23}$$

with

$$\begin{aligned} &c_0 = \mu^4\xi(\xi-1)(f_T-f_0) - \mu^2\xi a_2 - a_0, \qquad c_1 = -\mu^2\xi a_3 - a_1, \qquad c_2 = \mu^2(\xi-1)(f_T-f_0) - \frac{1}{2}a_2, \\ &c_3 = -\frac{1}{6}a_3, \qquad c_4 = \frac{\mu^2}{12}(\xi-1)(f_T-f_0), \qquad c_5 = 0, \qquad c_6 = \frac{1}{360}(f_T-f_0). \end{aligned} \tag{24}$$

Both for $n = 1$ and $n = 2$, let $w(s; a_i, f_T)$ be the general solution of Eq. (13). The six constants a_i, for $i = 0, 1, \ldots, 5$, are readily found from the boundary conditions (15)–(17). Let $w^*(s, f_T)$ be the solution of problem (13)–(17), then the deflection of the cantilever tip will be

$$w_T = w^*(1; f_T), \tag{25}$$

Substituting (20) into (25) gives the relation $w^*(1, f_T(w_T; \alpha, \beta)) = w_T$. It can be considered as the equation for seeking the required parameter α, if the electrostatic force is absent, or β under applied voltage. Then the critical parameters α^*, β^*, as well as the corresponding deflection w_T^* of the tip, can be determined from conditions (18).

6. Comparative analysis of different approaches

Although the approach based on the LDL and QDL models has proven itself well in studying the pull-instability of nanoswitches (Mikhasev et al., 2022), we will carry out a comparative analysis of calculations for tweezers performed using both the proposed and alternative methods (Bianchi et al., 2022). Here, we ignore the internal nonlocal effects setting $\xi = 1$ and $\mu = 0$, which corresponds to the problem statement in Bianchi et al. (2022). In Fig. 2, the critical vdW parameter α^* is depicted as the function of the critical tip deflection w_T^* for classical elastic behavior of the nanocantilever. Calculations were performed on the base of the LDL and QLD models and from the shooting methods (Bianchi et al., 2022) and presented by curves 1, 2, and 3, respectively. It can be observed that the QDL model approaches the numerical results of the shooting method better than the LDL model.

Fig. 3 displays the critical pull-in voltage parameter β^* versus the tip deflection w_T^* for various values of the vdW parameter α and for the fixed geometrical characteristic $k = 100$ at $\xi = 1$, $\mu = 0$. The four groups of lines marked by 1, 2, 3, and 4 correspond to values $\alpha = 0.0, 0.3, 0.6, 1.0$, respectively. The blue and red lines are plotted within the LDL and QDL models, respectively, while the green dotted lines are obtained by using the shooting method (Bianchi et al., 2022).

It is seen from Figs. 2 and 3 that all approaches give very close outcomes when the critical deflection w_T^* of the arm tip is small. However, the divergence of results grows together with the deflection w_T^*, for all that the curves constructed within the framework of the QDL model turn to be closer to results of the shooting method, the LDL model yielding lower values for both the vdW parameter α^* and the pull-in voltage β^*.

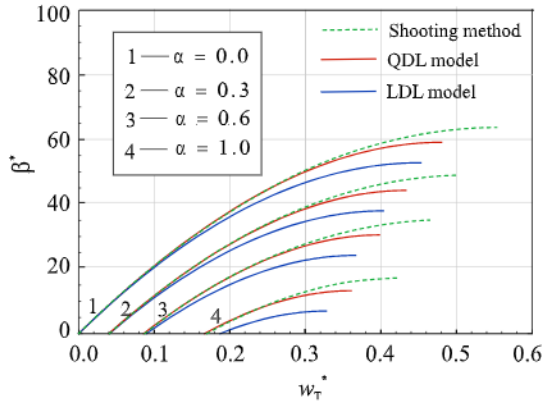

Fig. 3. The critical pull-in voltage parameter β^* versus the tip deflection w_T^* obtained on the base of the LDL and QDL models (blue and green lines, respectively) and from the shooting method (red dotted lines) (Bianchi et al., 2022) for classical elastic behavior of the nanocantilever and for four values of the vdW parameter α: (1) $\alpha = 0$, (2) $\alpha = 0.3$, (3) $\alpha = 0.6$, (4) $\alpha = 1$.

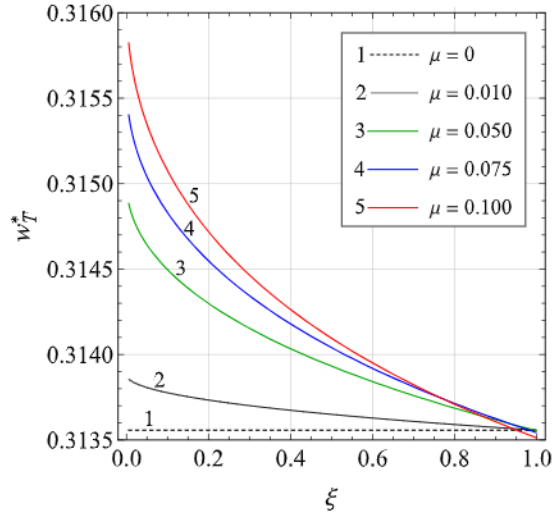

Fig. 4. Tip deflection w_T^* of the arm for a freestanding nanotweezer versus the local model fraction ξ evaluated within the LDL model for different dimensionless internal length scale parameter μ.

Having known the critical value of the vdW parameter from Fig. 2, one can estimate the critical geometrical parameters for the freestanding tweezers when the voltage is absent. From Eq. (12), we obtain the inequality

$$\frac{l^4}{g^{7/2}} < \frac{128EIr^{3/2}\alpha^*}{3At^2}, \tag{26}$$

which guarantees the stable position of the nanotweezer arms without sticking effect.

7. Freestanding tweezers taking into account nonlocal effects

We consider the freestanding nanotweezer ($\beta = 0$) accounting for the nonlocal effects. The critical tip deflections w_T^* versus the local model fraction ξ calculated within LDL and QDL models for various internal length scale parameters μ are shown in Figs. 4 and 5. It is seen that introducing the nonlocal phase in the constitutive law (8) leads to increasing the tip deflection. The smaller the local model fraction ξ, the greater the tip deflection w_T^* found on the base of both LDL and QDL approaches. Comparing Figs. 4 and 5 shows that for any fixed ξ, the QLD model gives a higher tip deflection than the LDL model.

Fig. 6 depicts the variation of the local model fraction ξ with the critical vdW parameter α^* obtained on the base of the LDL and QDL approaches (solid and dashed lines, respectively) for various values of the internal length scale parameter μ. As in the framework of the classical theory of elasticity considered in the previous item, the QDL model yields a higher critical value of the vdW parameter than the LDL model. When $\xi \to 0$, the critical value of α^* decreases and in the limit reaches a value corresponding to

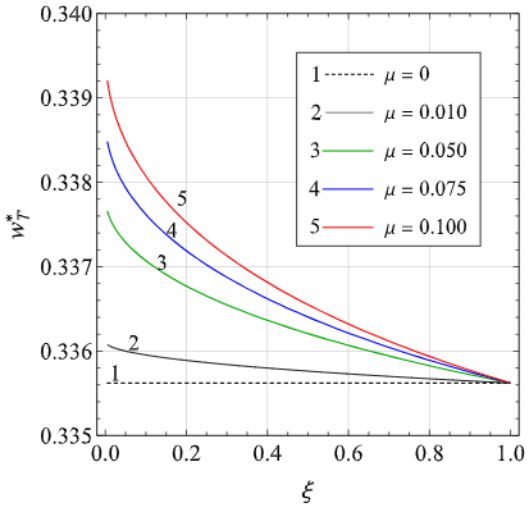

Fig. 5. Tip deflection w_T^* of the arm for a freestanding nanotweezer versus the local model fraction ξ evaluated within the QDL model for different dimensionless internal length scale parameter μ.

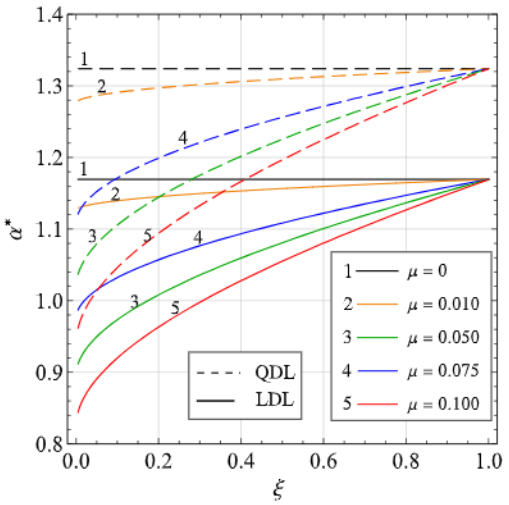

Fig. 6. Critical value of the vdW parameter α^* for a freestanding nanotweezer versus the local model fraction ξ evaluated within the LDL and QDL models (solid and dashed lines, respectively), for various dimensionless internal length scale parameter μ.

the purely nonlocal theory of elasticity for both the LDL and QDL models. If the internal length scale parameter μ becomes negligibly small, all curves corresponding to both models degenerate into the two straight lines (solid and dashed black lines) related to the classical theory of elasticity. Let us point out here the similarity of the reduction effects for the critical parameter α^* and the natural frequencies (Mikhasev & Nobili, 2020) for a cantilever nanobeam, induced by the nonlocal model fraction $\xi_2 = 1 - \xi$.

Within the nonlocal theory of elasticity, the restriction for geometrical parameters of the freestanding tweezers, which ensures the pre-buckling stable position of the arms, is again given by inequality (26).

8. Pull-in voltage taking into account nonlocal effects

Let us now consider the nanotweezer under the action of the attractive electrostatic forces ($\beta > 0$). The critical value β^* of the voltage parameter as well as the associated critical tip deflection w_T^* are determined from Eq. (18). Figs. 7 and 8 show the critical tip deflection and voltage parameter, respectively, versus the local model fraction ξ calculated within both LDL and QDL models for various values of the vdW parameter α and for the fixed geometrical ratio $k = 10$ and the dimensionless internal scale parameter $\mu = 0.05$. For voltage and deflection lower than their critical pull-in values, the behavior of the nanotweezer is stable. These limits define the tweezing range and thus the size of objects that can be manipulated by the nanotweezers. As above, the QDL model

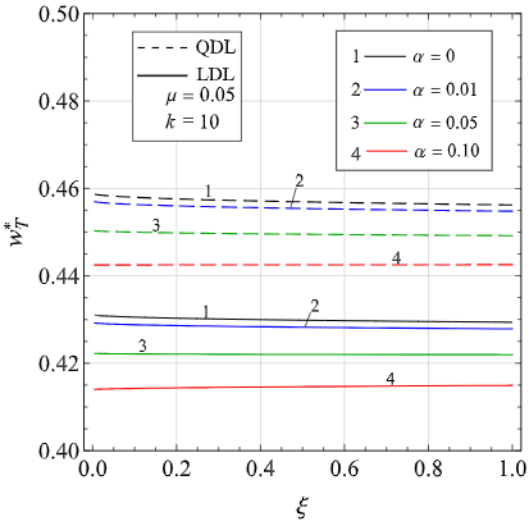

Fig. 7. Tip deflection w_T^* of the nanotweezer arm versus the local model fraction ξ evaluated within the LDL and QDL models (solid and dashed lines, respectively), for various values of the vdW parameter α and for the fixed geometric coefficient $k = 10$ and dimensionless internal length scale parameter $\mu = 0.05$.

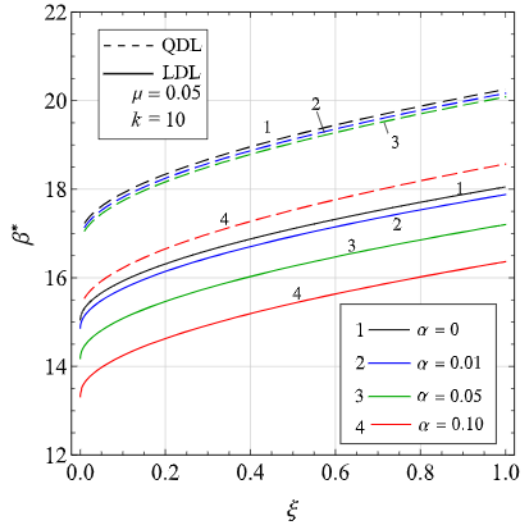

Fig. 8. Critical pull-in voltage parameter β^* versus the local model fraction ξ evaluated within the LDL and QDL models (solid and dashed lines, respectively), for various values of the vdW parameter α and for the fixed geometric coefficient $k = 10$ and dimensionless internal length scale parameter $\mu = 0.05$.

results in higher values of both the critical voltage and tip deflection for any value of the parameter ξ. It is interesting to note that varying the local model fraction ξ slightly affects the critical tip deflection for large values of the vdW parameter α, its increase leading to a barely noticeable decrease in the deflection only at very small values of the parameter α.

On the contrary, the critical voltage parameter β^* clearly grows up together with the parameter ξ, for any value of the vdW parameter α, thus showing that the nonlocal response of the material at the nanoscale has a significant influence on the pull-in voltage. The higher values of the pull-in voltage on both figures correspond to the limiting case when the effect of vdW forces becomes negligibly small. As the effects of the vdW forces come into play, the pull-in voltage is reduced consequently. Therefore, both nonlocal behavior and surface attractions may cause significant variations of the pull-in voltage, which must be taken into consideration to avoid device malfunctions.

The effects of the internal length scale parameter μ on the variations of the critical pull-in voltage parameter β^* with the local model fraction ξ are illustrated in Fig. 9 for $\alpha = 0.05$ and k =10, both for linear and quadratic models. It can be observed that the pull-in voltage decreases as the internal length scale parameter μ increases, especially for low values of the local model fraction ξ. However, the effect of μ on the pull-in voltage becomes vanishing small as ξ tends to 1. Again, the QDL model predicts higher pull-in voltages with respect to the LDL model.

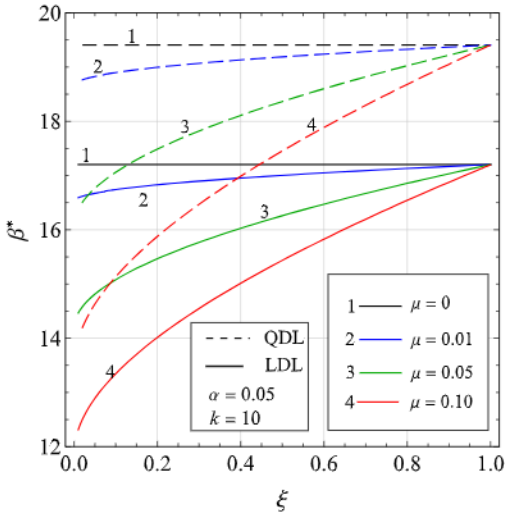

Fig. 9. Critical pull-in voltage parameter β^* versus the local model fraction ξ evaluated within the LDL and QDL models (solid and dashed lines, respectively), for various values of dimensionless internal length scale parameter μ and for the fixed geometric coefficient $k = 10$ and vdW parameter $\alpha = 0.05$.

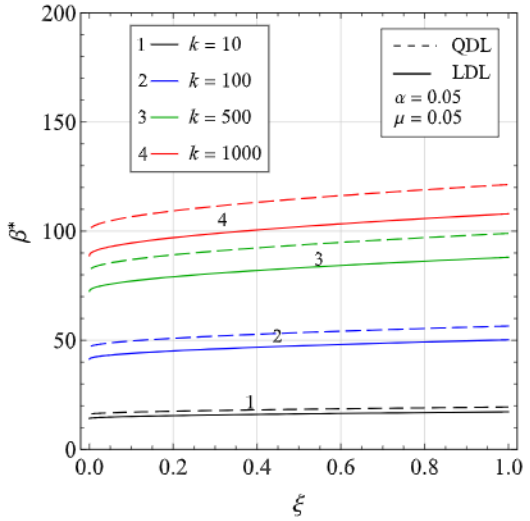

Fig. 10. Critical pull-in voltage parameter β^* versus the local model fraction ξ evaluated within the LDL and QDL models (solid and dashed lines, respectively), for various values of the geometric coefficient k and for the fixed dimensionless internal length scale parameter $\mu = 0.05$ and vdW parameter $\alpha = 0.05$.

The effects of the geometric coefficient k on the variations of the critical pull-in voltage parameter β^* with the local model fraction ξ predicted by both models are then depicted in Figs. 10 and 11, for $\mu = 0.05$ and for two different values of α, namely 0.05 and 1.0, respectively. One can see that the pull-in voltage generally increases with the geometric coefficient k, namely for a large gap. Moreover, the pull-in voltages predicted by the two models are close enough for low values of α and k, but their difference increases for large values of the vdW parameter α.

The variations of the voltage parameter β with the corresponding tip deflection w_T of the nanotweezer arm evaluated within the LDL and QDL models are presented in Fig. 12, for some values of the vdW parameter α and for the fixed geometric coefficient $k = 100$, for fixed dimensionless internal length scale parameter $\mu = 0.1$ and for vanishing local model fraction $\xi = 0$. The maxima of these variations correspond to the critical pull-in values β^* and w_T^*. These results show that the QDL model predicts pull-in parameters a bit larger than those derived by the LDL model, especially for large vdW parameter α. It must be observed that the initial deflection of the nanotweezer arms without any external voltage applied, namely for $\beta = 0$, increases with the vdW parameter α and approaches the critical pull-in deflection as α attains its critical value α^* for a freestanding nanotweezer.

To validate the assumption on the quadratic load distribution, in Fig. 13 we plotted the quadratic loading function in (19) for $n = 2$ (dashed blue lines) and the actual loading function in (14) evaluated by considering the deflection obtained from the QDL model (solid red lines), for three values of β, being the higher value close to the pull-in voltage parameter β^*. One can observe that

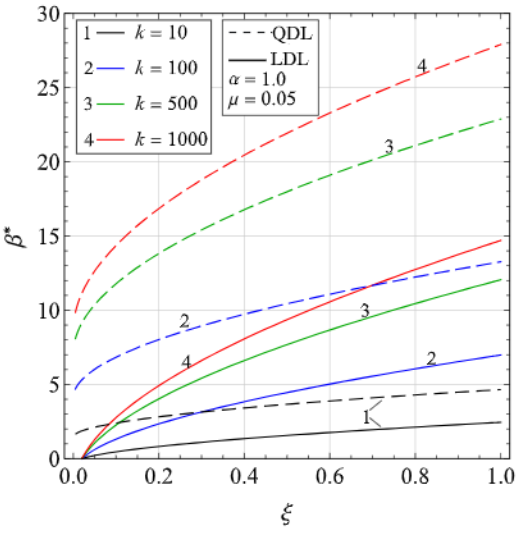

Fig. 11. Critical pull-in voltage parameter β^* versus the local model fraction ξ evaluated within the LDL and QDL models (solid and dashed lines, respectively), for various values of the geometric coefficient k and for the fixed dimensionless internal length scale parameter $\mu = 0.05$ and vdW parameter $\alpha = 1$.

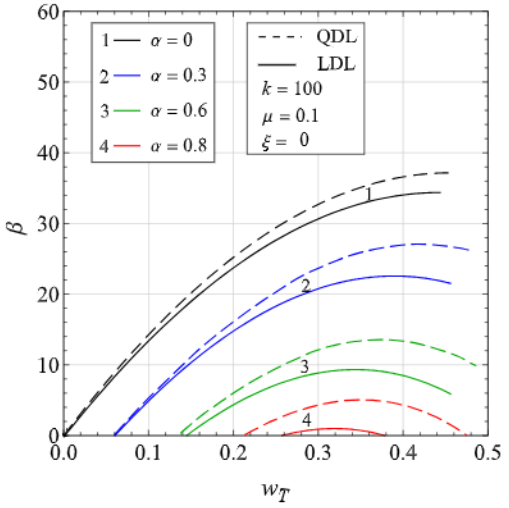

Fig. 12. Voltage parameter β versus the tip deflection w_T of the nanotweezer arm evaluated within the LDL and QDL models (solid and dashed lines, respectively), for various values of the vdW parameter α and for the fixed geometric coefficient $k = 100$, for fixed dimensionless internal length scale parameter $\mu = 0.1$ and local model fraction $\xi = 0$.

for each value of β the solid and dashed curves are quite close each other, thus proving the accuracy of the QDL model. In particular, for lower value of β the quadratic loading function turns out to be a bit lower than the actual loading function, whereas for high values of β the order is reversed. Therefore, the pull-in voltage provided by the QDL mode is a bit lower than the actual pull-in voltage. The linear loading distribution of the LDL model is always higher than the actual loading function, and they coincide only at the nanobeam edges for $s = 0$ and $s = 1$. Therefore, the pull-in voltage provided by the LDL mode is generally much lower than the actual pull-in voltage.

9. Conclusions and discussion

In this work, the pull-in voltage and the maximum static deflection of CNT nanotweezers are investigated by considering the effect of electrostatic and vdW forces, and nonlocal constitutive behavior of the material. Two size-dependent models are developed by using a TPNL constitutive model of the CNTs and assuming two simplified loading distributions along the arms, namely linear and quadratic. The analytical results attained here show that there are obvious changes in pull-in voltage and deflection as the constitutive behavior changes from local to nonlocal, as well as the effects of the vdW forces are increased. These contributions

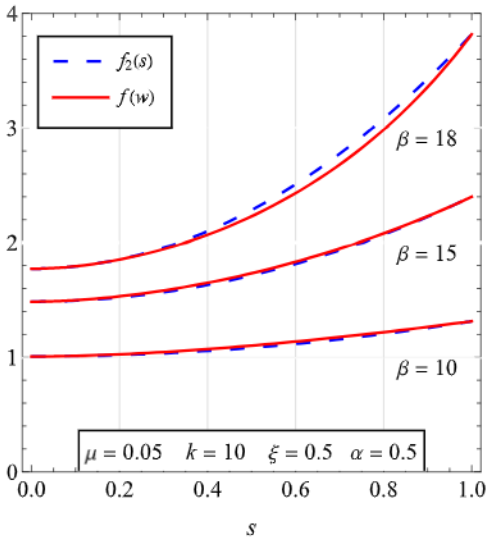

Fig. 13. Loading distribution along the nanotweezer arm defined by the quadratic function $f_2(s)$ in (19) and the actual distribution $f(w)$ in (14) calculated by considering the deflection w obtained from the QDL model, for three values of the voltage parameter β and for $\alpha = 0.5$, $k = 10$, $\mu = 0.05$, and $\xi = 0.5$.

cannot be overlooked if the system is required to achieve reliability and sensitivity to functionality at the nanoscale In conclusion, the use of the TPNL theory of elasticity for modeling nanotweezer behavior under electrostatic loadings has shed light on the significance of considering nonlocal effects at the nanoscale. The proposed analytical model can be used to accurately determine the required voltage for a desired gap distance. It has enhanced the understanding of the behavior of these devices at the nanoscale and has paved the way for more accurate predictions and design considerations in this field. Moreover, it provides a means to compare and validate further numerical investigations.

CRediT authorship contribution statement

Gennadi Mikhasev: Writing – review & editing, Writing – original draft, Supervision, Formal analysis, Conceptualization. **Enrico Radi:** Writing – review & editing, Writing – original draft, Software, Methodology, Investigation, Formal analysis. **Vyacheslav Misnik:** Visualization, Software, Investigation.

Declaration of competing interest

The authors declare that they have no known competing financial interests or personal relationships that could have appeared to influence the work reported in this paper.

Data availability

Data will be made available on request.

Acknowledgments

ER is grateful to the Italian “Gruppo Nazionale di Fisica Matematica” INdAM-GNFM for support.

References

Benvenuti, E., & Simone, A. (2013). One-dimensional nonlocal and gradient elasticity: closed-form solution and size effect. *Mechanics Research Communications*, *48*, 46–51.

Bianchi, G., Sorrentino, A., Radi, E., & Castagnetti, D. (2022). Electrostatic pull-in instability for tweezer architectures. *Meccanica*, *57*, 1767–1781. http://dx.doi.org/10.1007/s11012-022-01546-0.

Challamel, N., & Wang, C. (2008). The small length scale effect for a non-local cantilever beam: a paradox solved. *Nanotechnology*, *19*(34), Article 345703.

Chebakov, R., Kaplunov, J., & Rogerson, G. (2017). A non-local asymptotic theory for thin elastic plates. *Proceeding s of the Royal Society A. Mathematical, Physical and Engineering Sciences*, *473*(2203), Article 20170249.

Demir, C., & Civalek, Ö. (2017). On the analysis of microbeams. *International Journal of Engineering Science*, *121*, 14–33.

Eringen, A. C. (1984). *Theory of nonlocal elasticity and some applications*: *Technical report*, Princeton Univ NJ Dept of Civil Engineering.

Eringen, A. C. (2002). *Nonlocal continuum field theories*. Springer Science & Business Media.

Farrokhabadi, A., Koochi, A., Kazemi, A., & Abadyan, M. (2014). Effects of size-dependent elasticity on stability of nanotweezers. *Journal of Applied Mathematics and Mechanics*, *35*, 1573–1590.

Farrokhabadi, A., Mokhtari, J., Rach, R., & Abadyan, M. (2015). Modeling the influence of the casimir force on the pull-in instability of nanowire-fabricated nanotweezers. *International Journal of Modern Physics B. Condensed Matter Physics. Statistical Physics. Applied Physics.*, *29*(2), Article 1450245.

Farrokhabadi, A., Rach, R., & Abadyan, M. (2013). Modeling the static response and pull-in instability of CNT nanotweezers under the Coulomb and van der Waals attractions. *Physica E: Low-dimensional Systems and Nanostructures*, *53*, 137–145.

Fernandez-Saez, J., & Zaera, R. (2017). Vibrations of Bernoulli-Euler beams using the two-phase nonlocal elasticity theory. *International Journal of Engineering Science*, *119*, 232–248.

Kaplunov, J., Prikazchikov, D., & Prikazchikova, L. (2023). On integral and differential formulations in nonlocal elasticity. *European Journal of Mechanics. A. Solids*, *100*, Article 104497.

Khodabakhshi, P., & Reddy, J. (2015). A unified integro-differential nonlocal model. *International Journal of Engineering Science*, *95*, 60–75. http://dx.doi.org/10.1016/j.ijengsci.2015.06.006.

Kim, P., & Lieber, C. M. (1999). Nanotube nanotweezers. *Science*, *286*(5447), 2148–2150.

Lee, J., & Kim, S. (2005). Manufacture of a nanotweezer using a length controlled CNT arm. *Sensors and Actuators A: Physical*, *120*(1), 193–198.

Li, C., Yao, L., Chen, W., & Li, S. (2015). Comments on nonlocal effects in nano-cantilever beams. *International Journal of Engineering Science*, *87*, 47–57.

Malikan, M., Dastjerdi, S., Eremeyev, V., & Sedighi, H. (2023). On a 3D material modelling of smart nanocomposite structures. *International Journal of Engineering Science*, *193*, Article 103966. http://dx.doi.org/10.1016/j.ijengsci.2023.103966.

Menning, J., Eberhardt, O., & Wallmersperger, T. (2022). Grasping the little things: Modeling and simulation of the electromechanical behavior of individual carbon nanotubes and nanotweezers. *Carbon Trends*, *9*, Article 100192.

Miandoab, E. M., Yousefi-Koma, A., & Pishkenari, H. N. (2015). Nonlocal and strain gradient based model for electrostatically actuated silicon nano-beams. *Microsystem Technologies*, *21*, 457–464.

Mikhasev, G. (2021). Free high-frequency vibrations of nonlocally elastic beam with varying cross-section area. *Continuum Mechanics and Thermodynamics*, *33*, 1299–1312. http://dx.doi.org/10.1007/s00161-021-00977-6.

Mikhasev, G., & Nobili, A. (2020). On the solution of the purely nonlocal theory of beam elastcity as a limiting case of the two-phase theory. *International Journal of Solids and Structures*, *190*, 47–57. http://dx.doi.org/10.1016/j.ijsolstr.2019.10.022.

Mikhasev, G., Radi, E., & Misnik, V. (2022). Pull-in instability of a nanocantilever based on two-phase nonlocal theory of elasticity. *Journal of Applied and Computational Mechanics*, *8*(4), 1456–1466. http://dx.doi.org/10.22055/JACM.2022.40638.3619.

Pisano, A., Fuschi, P., & Polizzotto, C. (2021). Integral and differential approaches to Eringen's nonlocal elasticity models accounting for boundary effects with applications to beams in bending. *ZAMM-Journal of Applied Mathematics and Mechanics*, *101*(8), Article e202000152.

Rahaeifard, M., & Ahmadian, M. (2015). On pull-in instabilities of microcantilevers. *International Journal of Engineering Science*, *87*, 176–186. http://dx.doi.org/10.1016/j.ijengsci.2014.11.002.

Ramezani, A. (2011). Stability analysis of electrostatic nanotweezers. *Physica E: Low-dimensional Systems and Nanostructures*, *43*(10), 1783–1791.

Ramezani, A., Alasty, A., & Akbari, J. (2007). Closed-form solutions of the pull-in instability in nanocantilevers under electrostatic and intermolecular surface forces. *International Journal of Solids and Structures*, *44*, 4925–4941.

Romano, G., Barretta, R., Diaco, M., & de Sciarra, F. (2017). Constitutive boundary conditions and paradoxes in nonlocal elastic nanobeams. *International Journal of Mechanical Sciences*, *121*, 151–156.

Tavakolian, F., Farrokhabadi, A., SoltanRezaee, M., & Rahmanian, S. (2019). Dynamic pull-in of thermal cantilever nanoswitches subjected to dispersion and axial forces using nonlocal elasticity theory. *Microsystem Technologies*, *25*, 19–30.

Vaccaro, M., Pinnola, F., de Sciarra, F., & Barretta, R. (2021). Limit behaviour of Eringen's two-phase elastic beams. *European Journal of Mechanics. A. Solids*, *89*, Article 104315.

Yang, J., Jia, X., & Kitipornchai, S. (2008). Pull-in instability of nano-switches using nonlocal elasticity theory. *Journal of Physics D: Applied Physics*, *41*(3), Article 035103.

Zare, J., & Shateri, A. (2017). Instability threshold of rippled carbon nanotube nanotweezers in the low vacuum gas flow incorporating Dirichlet and Neumann modes of casimir energy. *Physica E: Low-dimensional Systems and Nanostructures*, *90*, 67–75.

Zeighampour, H., & Tadi Beni, Y. (2014). Cylindrical thin-shell model based on modified strain gradient theory. *International Journal of Engineering Science*, *78*, 27–47.

Zhang, W.-M., Yan, H., Peng, Z.-K., & Meng, G. (2014). Electrostatic pull-in instability in MEMS/NEMS: A review. *Sensors and Actuators A: Physical*, *214*, 187–218.